Journal of Ceramic Processing Research. Vol. 21, No. 1, pp. 42~49 (2020)
(Received 12 July 2019, Received in revised form 27 September 2019, Accepted 7 October 2019)
https://doi.org/10.36410/jcpr.2020.21.1.42

J O U R N A L O F
Ceramic Processing Research

Influence of surface roughness on the efficiency of a flexible organic solar cell

Se Hoon Kim[a], Deuk Yong Lee[b], and Young-Jei Oh[a,c,*]
[a]*Opto-electronic Materials & Devices Research Center, Korea Institute of Science and Technology, Seoul 02792, Korea*
[b]*Department of Biomedical Engineering, Daelim University, Anyang 13916, Korea*
[c]*Department of Nano Material Science and Engineering, Korea University of Science and Technology, Daejeon 34113, Korea*

Organic solar cells (OSCs) without an over-coating layer, consisting of a silver nanowire (AgNW) transparent electrode, a poly(3,4-ethylenedioxythiphene):poly (styrenesulfonate) (PEDOT:PSS) layer, a poly(3-hexylthiophene-2,5-diyl):the [6,6]-phenyl C61 butyric acid methyl ester (P3HT:PCBM) active layer, a LiF/Al electron collecting, and a top electrode, were successfully fabricated in order to investigate the effect of surface roughness on the efficiency of OSCs. The AgNW transparent electrode on acryl resin coated polyethylene terephthalate (PET) film was prepared through the filtration/transfer method. Sheet resistance of 30 Ω^{-1} and surface roughness of 10.5 nm were detected. After coating the PEDOT:PSS hole transfer layer and the P3HT:PCBM active layer at 1000 rpm on the AgNW/PET transparent electrode, the surface roughness was reduced dramatically. However, open circuit voltage, short circuit current density, fill factor, and power conversion efficiency decreased as the coating speed was raised during the formation of the PEDOT:PSS layer and the P3HT:PCBM active layer due to the deterioration of the surface roughness. The surface roughness was determined to be crucial for the output performance of OSCs.

Key words: silver nanowire (AgNW), filtration/transfer method, spin coating, surface roughness, organic solar cell (OSC)

Introduction

Although indium tin oxide (ITO) is widely used as a transparent electrode material due to its excellent electrical conductivity and transmittance of 85% or more in the visible light region, its high price and a shortage of indium resources limit its widespread use [1-14]. In addition, when the ITO film on a flexible substrate is bent, it becomes cracked or broken [4, 5]. Its brittleness and high surface resistance make it difficult to use in flexible electronic devices. An increased demand for flexible electronic devices has fueled the development and introduction of new transparent conducting materials such as conducting polymers, carbon nanotubes (CNTs), graphene, highly conductive poly(3,4-ethylenedioxythiphene):poly (styrenesulfonate) (PEDOT:PSS), and metal nanowire as alternatives to ITO [1-9]. The transparent electrode material is used for photo-electronic devices such as organic light-emitting diodes and organic solar cells (OSCs). Solar cell technology should provide a safe, clean, and most affordable potential energy source among renewable energy technologies such as dye-sensitized solar cells [15-18]. The OSC has several advantages, which include low cost, renewability, and energy harvest due to high power conversion efficiency [4].

*Corresponding author:
Tel : +82-2-958-5553
Fax: +82-2-958-5554
E-mail: youngjei@kist.re.kr

Among the alternatives, metal nanowires possessing excellent transmittance, sheet resistance, and flexibility can be made into a large area at a low cost compared to organic conducting polymers [5]. In this work, flexible OSCs are fabricated using silver nanowires (AgNWs) as the transparent electrode on the substrate. AgNWs have been used as ITO in OSCs due to their excellent conductivity, transmittance, and flexibility. The disadvantages of AgNWs, such as low adhesion force on the substrate and low resistance to corrosion, can be overcome by embedding AgNWs strongly in a polymer surface [1]. The performance of the OSCs employing AgNWs is then evaluated as a function of surface roughness.

Experimental Details

To prepare an AgNW dispersion solution suitable for the spraying method and filtration/transfer method, isopropyl alcohol, ethylene glycol, ethylene glycol monoethyl ether and distilled water were used. The AgNW dispersion solution was modified by adding a binder (hydroxy propylmethyl cellulose) and a dispersant (Zonyl FSO-100, DuPont) to prevent aggregation of the dispersed AgNW during drying [8]. The bottom of the spray coating equipment, as shown in Fig. 1(a), was heated to 80 °C. Then, the substrate was placed on the heated bottom surface and it was fixed using a vacuum. The dispersed AgNW was placed in a storage container for extrusion of the spray equipment. The liquid was

Fig. 1. Photographs of (a) spray coater and (b) filtration apparatus.

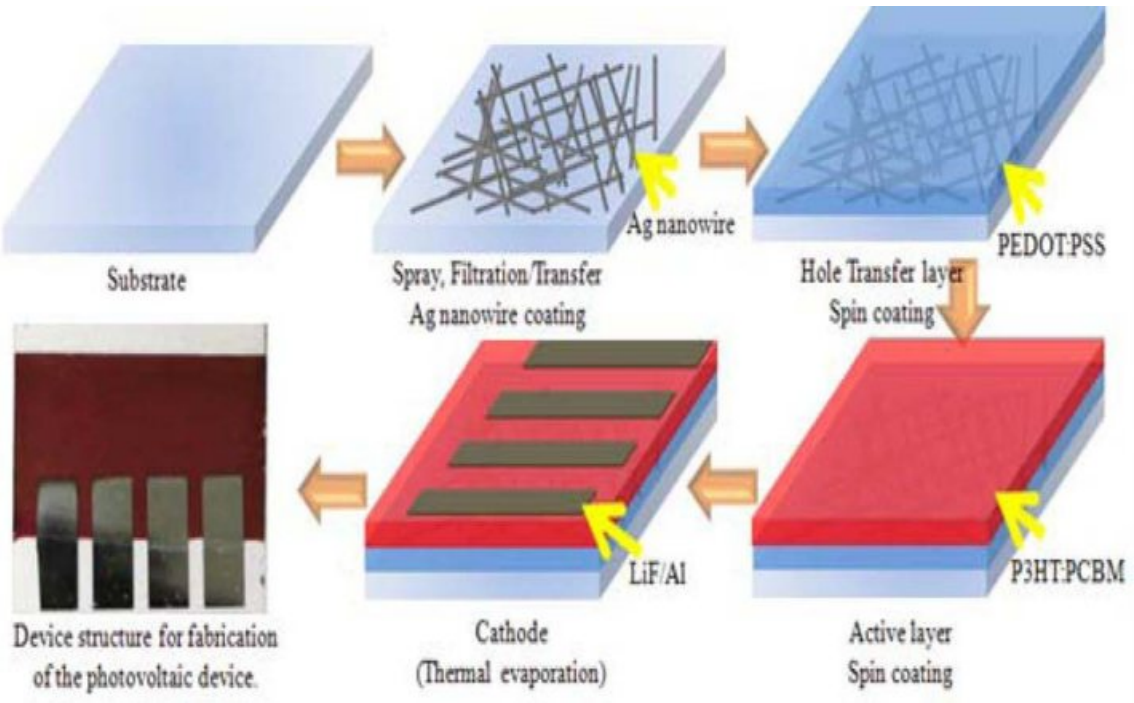

Fig. 2. Fabrication procedure of the OSCs.

subjected to an extrusion pressure of 0.01 MPa and an air extrusion pressure of 0.01 MPa. The X and Y axis movement speed was 20 mm/sec and 2 mm/sec, respectively. The transparent electrode was fabricated by spray-coating the AgNW on the substrate.

The AgNW dispersed solution, which was used for the filtration/transfer method (Fig. 1(b)), was poured into a Teflon filter paper using a vacuum pump to leave only AgNWs on the filter paper. The substrate and the AgNW remaining on filter paper were placed on the heated laminator at 120 ºC and then pressed for 5 min at 0.1 kg_f/cm^2 to form a transparent electrode.

The device, as depicted in Fig. 2, consists of an AgNW transparent electrode, a PEDOT:PSS as the hole collecting layer, a poly(3-hexylthiophene-2,5-diyl):the [6,6]-phenyl C61 butyric acid methyl ester (P3HT:PCBM) active layer, and a LiF/Al electron collecting and top electrode [8]. Prior to spin-coating, the AgNW transparent electrode was UV treated for 15 min for better coating. A PEDOT:PSS bilayer (Clevios™ PH 1000 and Al 4083, respectively) was spin-coated on the AgNW transparent electrode as a hole transfer

layer. The PEDOT:PSS was mixed with methanol at a 1: 1 volume ratio and this solution was spun at various speeds in the range of 1,000 rpm, 2,000 rpm, 3,000 rpm to 4000 rpm for 45 s, respectively, and subsequently dried on a hot plate for 30 min at 110 ºC.

P3HT and PCBM (1:0.6 weight ratio) were melted in 1 mL of chlorobenzene as an electron transport layer. The mixture was spin-coated at 1,000 rpm, 2,000 rpm, and 3000 rpm, respectively, after which it was dried on a hot plate for 10 min at 150 ºC. Finally, the LiF/Al electron-collecting top electrode was subjected to thermal evaporation to fabricate the final OSCs. The thickness of LiF and Al were 6 Å and 100 nm, respectively.

Results and Discussion

A dispersion solution of AgNW suitable for the spray method and the filtration/transfer method was examined because the electrical and optical properties were measured differently due to the agglomeration between the AgNWs. SEM images in Fig. 3(a) show high linearity and no cohesion between the AgNWs, which is suitable for the fabrication of transparent electrodes [8]. XRD results revealed that the peaks in the AgNW were consistent with (111), (200), and (220) planes from the standard powder pattern of Ag (JCPDS-04-0783), as shown in Fig. 3(b). The crystal structure of AgNWs was a face-centered cubic structure.

Transmittance of AgNW electrode on glass and PET substrates is shown in Fig. 4. The transmittance of the transparent electrode fabricated through the transfer method and the spray coating method on the PET film coated with acryl resin was 85% and 87%, respectively. The transmittance of the electrode prepared by the transfer method and the spray coating method on the glass substrate was 90% and 93%, respectively. The transmittance of the AgNW transparent electrodes was always higher than 85%, regardless of the substrate type and the coating method. Conventional transparent electrodes using ITO had a high transmittance of 85% in the visible light region and a low sheet resistance (30 Ω^{-1}) [4]. The AgNW transparent electrode was highly suitable for an alternative transparent electrode of ITO.

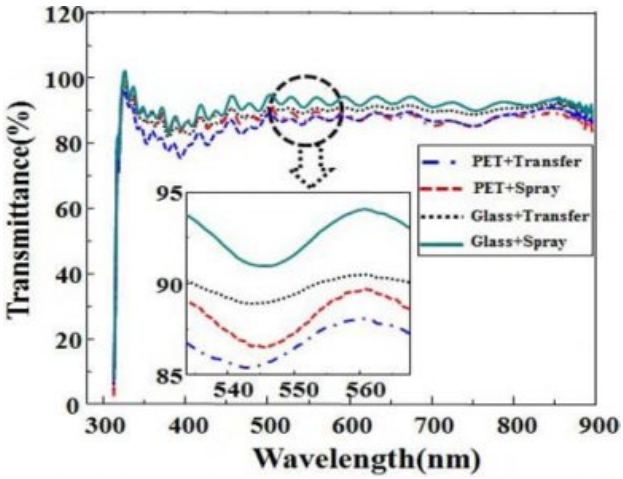

Fig. 4. Transmittance of AgNW electrode on the glass and PET substrates prepared by spray and transfer coating methods.

Table 1 Sheet resistance and surface roughness of OSCs on glass and PET with different coating methods

Type	Sheet resistance (Ω^{-1})	Surface roughness (nm)
Glass + spray	90	20.8
Glass + transfer	70	18.5
PET + spray	40	15.5
PET + transfer	30	10.5

Sheet resistance and surface roughness are summarized in Table 1. The surface roughness of a transparent electrode on acryl resin coated PET film, as displayed in Figs. 5 and 6, was slightly improved from 15.5 nm to 10.5 nm when the transparent electrode was prepared using the transfer method rather than the spray coating method. It was reported that the enhanced surface

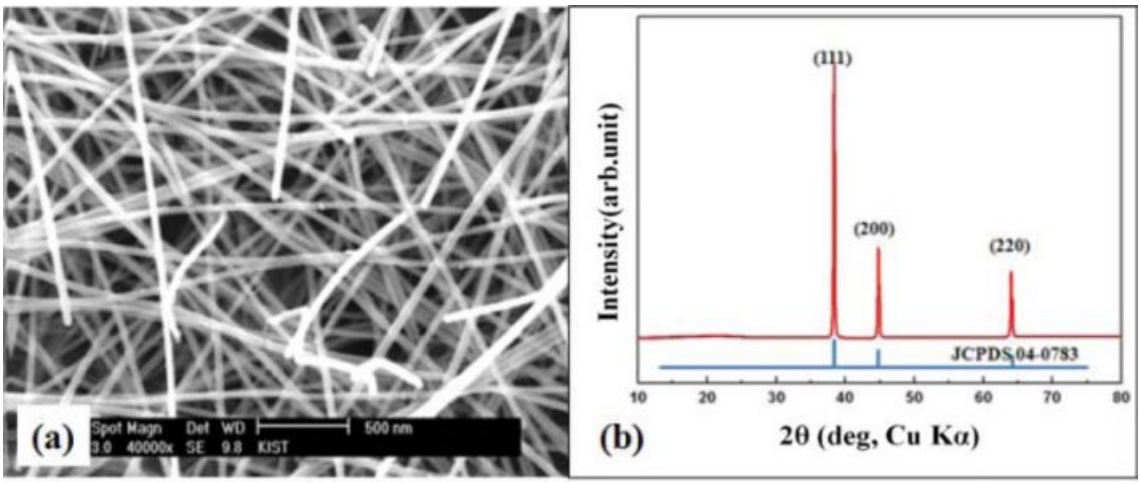

Fig. 3. (a) SEM image and (b) XRD diffraction of silver nanowires.

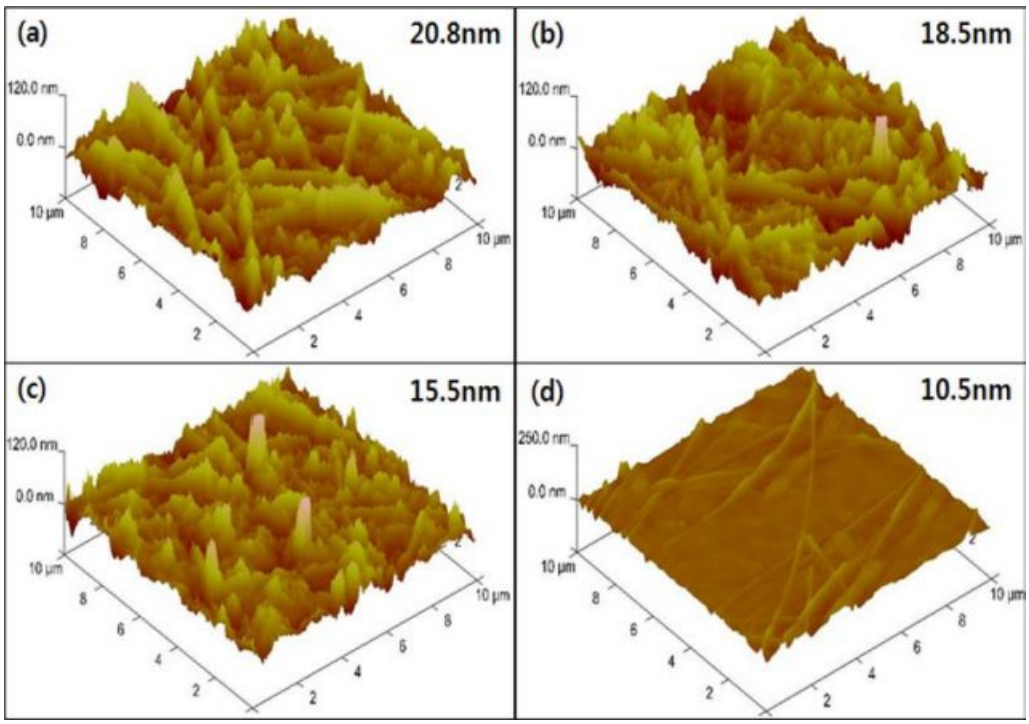

Fig. 5. AFM images of AgNW electrodes prepared by different substrate and coating method: (a) glass/spray, (b) glass/transfer, (c) PET/spray, and (d) PET/transfer.

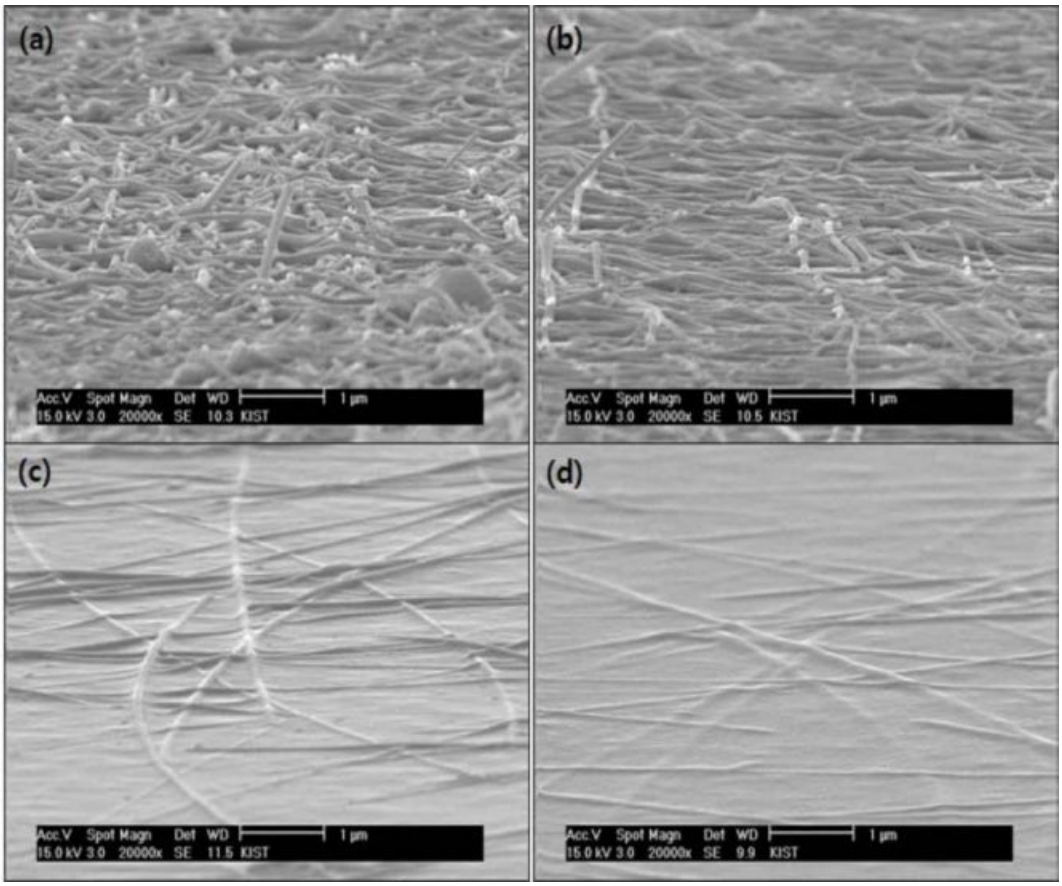

Fig. 6. SEM images of AgNW layers on (a,b) glass and (c,d) PET substrates prepared by (a,c) spray and (b,d) transfer method, respectively.

roughness of the AgNW mesh film could prevent an undesired leakage current path, leading to an improvement in device yield and reproducibility [9]. In addition, the acrylic resin buffer layer significantly strengthened the adhesion of AgNW mesh to the PET substrate. The roughness of the transparent electrode was dramatically deteriorated – from 10.5 nm to 18.5 nm – when it was coated on glass through the transfer method. The transfer method was found to be a better method than the spray coating method regardless of the substrate type. The sheet resistance of a transparent electrode on acryl resin coated PET film prepared through the transfer method and spray coating method was 30 Ω^{-1} and 40 Ω^{-1}, respectively. The sheet resistance rose significantly to 90 Ω^{-1} when both the spray coating method and the glass substrate were employed. Improved surface roughness was essential for efficient flexible OSC due to low sheet resistance. In the present study, the AgNW transparent electrode on acryl resin coated PET film prepared through the transfer method was investigated.

The PEDOT:PSS hole transfer layer was fabricated by varying the speed of the spin coater from 1,000 rpm to 4,000 rpm. The surface roughness of the hole transfer layer rose dramatically from 6.79 nm to 13.4 nm as the speed increased from 1,000 rpm to 4,000 rpm, as shown in Figs. 7 and 8. As the rotational speed of the spin coating increased, the thickness of the hole transfer layer became thinner because the flexible substrate was slightly bent at higher speeds. The surface roughness of the layer was then deteriorated as the speed increased because thin film was not uniformly formed due to the flexible PET film.

After coating PEDOT:PSS at 1,000 rpm on AgNW/PET transparent electrode, the surface roughness was observed by spin-coating the P3HT:PCBM active layer as a function of speed (1,000~4,000 rpm), as depicted in Fig. 9. The surface roughness of the active layer (2.93 nm, 3.64 nm) coated at speeds of 1,000 rpm and 2,000 rpm was much lower than that (6.79 nm) of PEDOT:PSS layer coated at 1,000 rpm. However, it rose dramatically as the speed increased. For OSCs using glass substrate, a vacuum was used to fix the rigid substrate when using the spin coater. On the other hand, when the flexible PET substrate was fixed using a vacuum, the film may be slightly bent due to the vacuum force. Therefore, the thin film was formed thicker than the curvature of the active layer thin film having the lowest surface roughness, resulting in an improved surface roughness. As spinning speed increased (3000~4000 rpm), the active layer became thinner. The thin film was not formed uniformly due to the warping of the substrate, so the surface roughness was measured as high.

I-V characteristics of the flexible OSCs containing the hole transfer layer and the active layer prepared at various speeds are shown in Fig. 10. The efficiency of the OSCs fabricated by coating the active layer at a speed of 1,000 to 4,000 rpm on the specimen coated with the hole transfer layer at 1,000 rpm is listed in Table 2. The reference device with the ITO electrode exhibited an open circuit voltage (V_{oc}) of 0.619 V, a

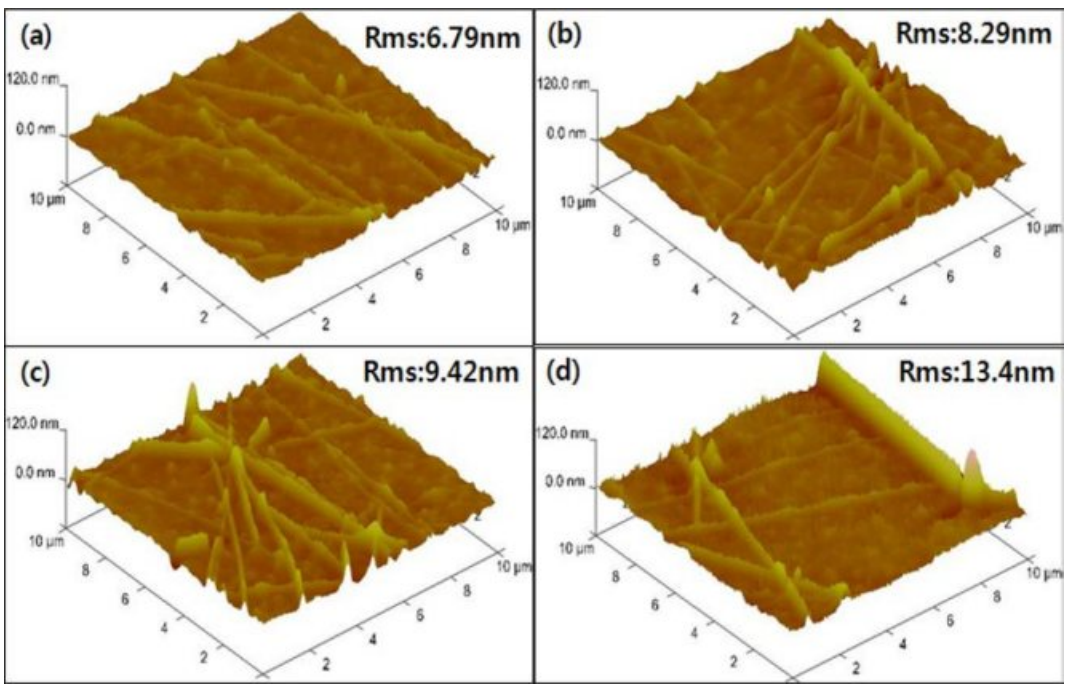

Fig. 7. AFM images of the hole transfer layer as a function of the coating speed: (a) 1000 rpm, (b) 2000 rpm, (c) 3000 rpm, and (d) 4000 rpm, respectively.

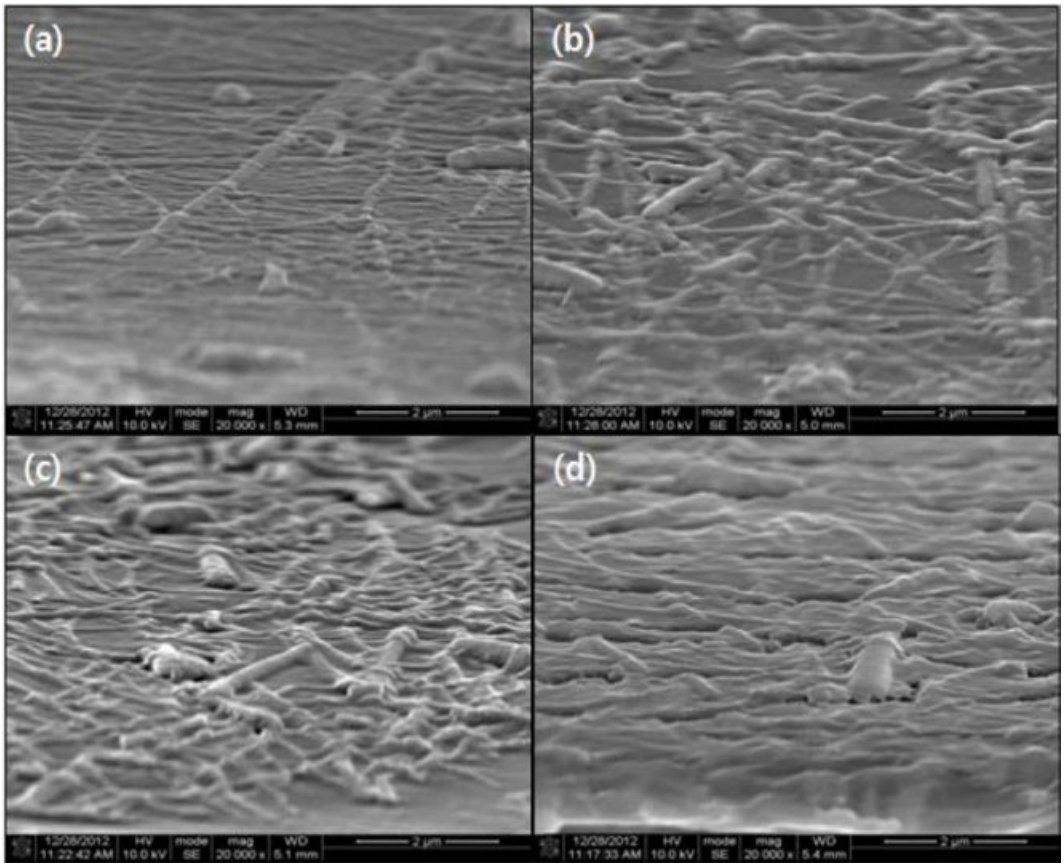

Fig. 8. SEM images of the hole transfer layers prepared by various speed: (a) 1000 rpm, (b) 2000 rpm, (c) 3000 rpm, and (d) 4000 rpm, respectively.

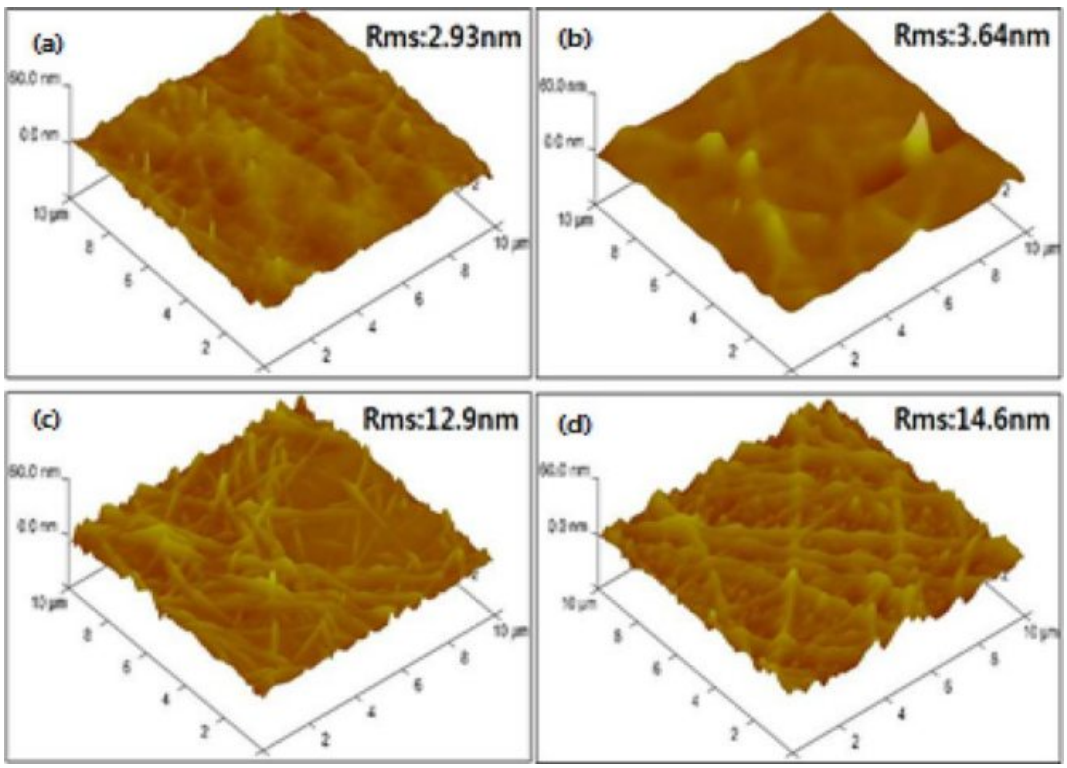

Fig. 9. AFM images of the active layers coated on the hole transfer layer prepared at a speed of 1000 rpm. The active layers were prepared by varying the speed: (a) 1000 rpm, (b) 2000 rpm, (c) 3000 rpm, and (d) 4000 rpm, respectively.

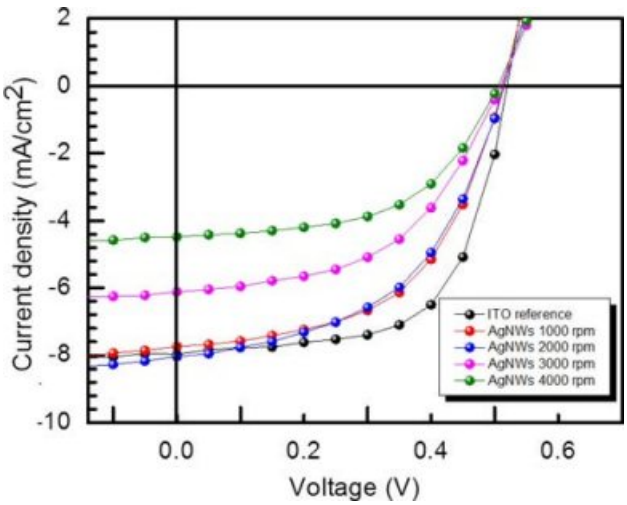

Fig. 10. I-V characteristics of the AgNWs/PEDOT:PSS/P3HT:PCBM/Lif:Al OSCs prepared by different coating speed.

Table 2 Performance of OSCs with the P3HT:PCBM active layer with various coating speeds

Electrode preparation	V_{oc} (V)	Jsc (mA/cm^2)	FF	h (%)
ITO	0.619	8.047	0.651	3.247
1000 rpm	0.612	7.930	0.568	2.761
2000 rpm	0.613	7.591	0.546	2.545
3000 rpm	0.609	6.244	0.538	2.409
4000 rpm	0.606	4.557	0.572	1.587

short circuit current (J_{sc}) of 8.047 mA/cm^2, a fill factor (*FF*) of 0.651, and a power conversion efficiency (*h*) of 3.247%, respectively [5, 15]. In comparison, the devices with the AgNW electrode fabricated by coating the active layer at 1,000 rpm showed V_{oc} of 0.612 V, J_{sc} of 7.930 mA/cm^2, *FF* of 0.568, and *h* of 2.761%, respectively. Although flexible OSCs were successfully fabricated, the power conversion efficiency was relatively low because there was no over-coating layer [5]. An over-coating layer and protection layer for the AgNWs using conducting polymers and oxides was employed to lower the surface roughness and improve the efficiency. But to simplify the process, no over-coating layer was used. As the rotation speed rose, V_{oc}, J_{sc}, *FF*, and *h* decreased, likely due to the deterioration of the surface roughness. As the speed increased, J_{sc} and *h* became lower due to the difference in hardness between glass and the PET substrate. Since the glass substrate is rigid, the substrate was not warped due to the vacuum applied to the spin coater to hold the substrate during coating, resulting in an improved surface roughness at 4,000 rpm. However, the PET substrate was slightly bent during the coating due to the vacuum and the speed. OSCs using PET substrate were believed to have an improved surface roughness due to the thick and smooth film of the hole transfer layer and the active layer prepared at 1,000 rpm. Higher J_{sc} and *h* were obtained at a low speed of 1,000 rpm due to the reduction in resistance, and there was excellent hole injection due to the improved surface roughness.

Flexible OSCs were fabricated using AgNWs as the transparent electrode on the PET substrate. The power conversion efficiency of OSCs using AgNWs was enhanced by using the over coating layer, resulting in an improved surface roughness [5]. However, the over coating layer had a disadvantage in that it cannot be applied to a large area and involved very complicated processes. The effect of surface roughness on the power conversion efficiency of the OSCs without the over coating layer was studied in the present study. The OSCs was prepared using the acryl resin coated PET substrate through the filtration/transfer method. The sheet resistance of 30 Ω^{-1} and the surface roughness of 10.5 nm were obtained, as listed in Table 1. The hole transfer layer (PEDOT:PSS) and the P3HT:PCBM active layer were prepared at 1000 rpm, leading to an enhanced surface roughness. The best performance of the OSCs prepared at low speed was observed. It could be concluded that the surface roughness was mainly attributed to the output performance of the OSCs.

Conclusions

A simple method for fabricating flexible OSCs, consisting of an AgNW transparent electrode, a hole transfer layer, an active layer, a LiF/Al electron collecting, and a top electrode was proposed by using AgNWs to replace ITO OSCs. The AgNW transparent electrode on acryl resin coated PET film was manufactured using the filtration/transfer method. After spin-coating the PEDOT:PSS layer and the P3HT:PCBM active layer at 1,000 rpm on AgNW/PET transparent electrode, an improved surface roughness was achieved. The OSCs with the AgNW electrode exhibited a relatively low V_{oc} of 0.612 V, J_{sc} of 7.930 mA/cm^2, *FF* of 0.568, and *h* of 2.761%. However, V_{oc}, J_{sc}, *FF*, and *h* decreased as the coating speed was increased during the formation of the hole transfer layer and the active layer due to undesired leakage current caused by higher surface roughness. The surface roughness was determined to be crucial for the output performance of OSCs. The AgNW transparent electrode was highly suitable for an alternative transparent electrode of ITO in OSCs.

References

1. C.-L. Kim, C.-W. Jung, Y.-J. Oh, and D.-E. Kim, NPG Asia Mater. 9 (2017) e438.
2. C.W. Tang, Appl. Phys. Lett. 48 (1986) 183-185.
3. J.Y. Kim, K. Lee, N.E. Coates, D. Moses, T. Nguyen, M. Dante, and A.J. Heeger, Science 317 (2007) 222-225.
4. C. Lee, R. Pandey, B. Wang, W. Choi, D. Choi, and Y.-J. Oh, Sol. Energy Mater. Sol. Cells 132 (2015) 80-85.
5. B.-Y. Wang, E. Lee, Y.-J. Oh, and H.W. Kang, RSC Adv. 7 (2017) 52914-52922.

6. B.J. Wiley, Y. Chen, J.M. McLellan, Y. Xiong, Z. Li, D. Ginger, and Y. Xia, Nano Lett. 7[4] (2007) 1032-1036.
7. C.J. Orendorff, L. Gearheart, N.R. Jana, and C.J. Murphy, Phys. Chem. Chem. Phys. 8 (2006) 165-170.
8. Y. Sun, B. Gates, B. Mayers, and Y. Xia, Nano Lett. 2 (2002) 165-168.
9. B.-Y. Wang, T. Yoo, J. Lim, B. Sang, D. Lim, W. Choi, D.K. Hwang, and Y.-J. Oh, Small 11 (2015) 1905-1911.
10. J. Xue, S. Uchida, B.P. Rand, and S.R. Forrest, Appl. Phys. Lett. 85 (2004) 5757-5759.
11. S.I. Na, S.S. Kim, J. Jo, and D.Y. Kim, Adv. Mater. 20 (2008) 4061-4067.
12. J. Xue, B.P. Rand, S. Uchida, and S.R. Forrest, Adv. Mater. 17 (2005) 66-71.
13. M. Vosgueritchian, D.J. Lipomi, and Z. Bao, Adv. Funct. Mater. 22 (2012) 421-428.
14. H. Hoppe and N.S. Saciciftci, J. Mater. Res. 19 (2004) 1924-1945.
15. Y. Kim, I. Lee, Y. Song, M. Lee, B. Kim, N. Cho, and D.Y. Lee, Electron. Mater. Lett. 10[2] (2014) 445-449.
16. D. Vikraman, A.A. Arbab, S. Hussain, N.K. Shrestha, S.H. Jeong, J. Jung, S.A. Patil, and H. Kim, ACS Sustainable Chem. Eng. 7 (2019) 13195-13205.
17. D.Y. Lee, H. Cho, D. Kang, J. Kang, M. Lee, B. Kim, and N. Cho, J. Korean Ceram. Soc. 51 (2014) 362-366.
18. S. Alwin, X.S. Shajan, K. Karuppasamy, and K.G.K. Warrier, Mater. Chem. Phys. 196 (2017) 37-44.